# *Rapid and Robust Detection Methods for Poison and Microbial Contamination*



**Citation:** Hoehl, Melanie M. et al. "Rapid and Robust Detection Methods for Poison and Microbial Contamination." Journal of Agricultural and Food Chemistry 60.25 (2012): 6349–6358.

**As Published:** http://dx.doi.org/10.1021/jf300817h

**Publisher:** American Chemical Society (ACS)

**Persistent URL:** http://hdl.handle.net/1721.1/80863

**Version:** Author's final manuscript: final author's manuscript post peer review, without publisher's formatting or copy editing

# Rapid and robust detection methods for poison and microbial contamination

*Melanie M. Hoehl,[1,2,*] Peter J. Lu,[3] Peter Sims,[4] and Alexander H. Slocum[1]*

[1] Department of Mechanical Engineering, MIT, Cambridge, MA 02139, USA

[2] Harvard-MIT Division of Health Sciences and Technology, Cambridge MA 02139 USA

[3] Department of Physics and SEAS, Harvard University, Cambridge, MA 02138 USA

[4] Columbia Initiative in Systems Biology, Department of Biochemistry and Molecular Biophysics, Columbia University Medical Center, New York, NY 10032, USA

* to whom correspondence should be addressed: hoehl@mit.edu

ABSTRACT. Real-time on-site monitoring of analytes is currently in high demand for food contamination, water, medicines and ingestible household products that were never tested appropriately. Here we introduce chemical methods for rapid quantification of a wide range of chemical and microbial contaminations using a simple instrument. Within the testing procedure, we used a multi-channel, multisample UV/vis spectrophotometer/fluorometer that employs two frequencies of light simultaneously to interrogate the sample. We present new enzyme- and dye-based methods to detect (di-)ethylene glycol in consumables above 0.1 wt% without interference and alcohols above 1 ppb. Using DNA intercalating dyes we can detect a range of pathogens (E. coli, Salmonella, Cholera and a model for malaria) in water, foods and blood without background signal. We achieved universal scaling independent of pathogen size above $10^4$ CFU/ml by taking advantage of the simultaneous measurement at multiple wavelengths. We can detect contaminants directly, without separation, purification, concentration or incubation. Our chemistry is stable to ±1% for more than three weeks without refrigeration, and measurements require less than five minutes.

KEYWORDS. UV absorption, fluorescence, detection, ethylene glycol, diethylene glycol, malaria, food pathogens, Salmonella, E.coli, Cholera.

MANUSCRIPT TEXT.

**Introduction:**

Contamination of food, water, medicine and ingestible household consumer products is a public health hazard that episodically causes thousands of deaths, and each year sickens millions worldwide.[1,2] For example, lower-cost ethylene glycol (EG) and diethylene glycol (DEG) have been substituted for the non-toxic glycerol, propylene glycol and polyethylene glycol, which are often used in medicines, household products, and foods.[3,4] Ingestion of even a small amount of EG or DEG can result in central nervous system depression, cardiopulmonary compromise, and kidney failure.[5,6,7,8] A longstanding problem that led to the 1938 Food, Drug and Cosmetic Act, establishing the modern drug-approval process within the United States Food and Drug Administration (FDA).[9] DEG contamination still remains a serious hazard today.[3] In the last 15 years, episodes of DEG poisoning have killed hundreds particularly in developing countries.[10-21,5,8,9] In addition to chemical poisoning, contamination of food and water by microbes such as E. coli and E. salmonella in food[2,22-25] or V. cholera in water[26,27] sickens millions (see SOM for recent contamination data).

Existing laboratory methods to detect many common relevant chemicals and pathogens (such as GC, MS, optical spectroscopy or electrochemistry[5,31,33-36]) require specialized scientific equipment, a stable laboratory environment, a continuous refrigeration chain for reagents or antibodies, and/or specially trained staff[28-33], all of which are expensive and generally preclude their use at the location of an outbreak or natural disaster[34]. Any detector for field use should rely on a simpler, more mechanically robust technology. There has thus been an effort to develop field-deployable diagnostic technologies (e.g. microfluidic, nanotechnology or surface plasmon resonance methods) that can be used outside a stable laboratory environment. For the past 7

years, this has lead to numerous publications about early stage technologies[33]. However, many of these technologies lack robustness, ease-of-use in the field and are usable for a single disease application only.[33]

Here we introduce robust chemical methods and a simple instrument to rapidly quantify a wide range of chemical and microbial contaminations. We employed far-field optical detection, which is particularly practical because it does not require physical contact with the sample. Instead of using a commercial spectrophotometer, we developed a low-cost detection device to perform our tests (see SOM). The device achieves robustness and high sensitivity by concurrently detecting UV absorption and fluorescence. The use of an optical readout allows it to be applicable for the detection of a range of analytes. In this paper, we focus on the enzyme- and dye-based methods to quantify the concentration of several chemical contaminants and microbial pathogens in a wide range of household products, medicines, foods and blood components.

We developed or procured assays for detecting different poisons shown in Table 1. These have been known to appear at all levels above those deemed safe by the U.S. FDA and the European Community.[10,28] We also measured the concentration of a range of primary alcohols in water, as alcohol in groundwater is a sign of gasoline spills or leaks. In addition, using DNA intercalator dyes, we measured the concentration of pathogenic microorganisms in common food materials that ordinarily contain little DNA, including E. salmonella in egg white, E. coli in milk, and V. cholera in water, at levels known to cause symptoms. Finally, we used yeast with a genome size comparable to that of Plasmodium, and quantified its concentration in a hematocyte suspension, as a rudimentary model for the detection of blood parasites, such as malaria. It is essential that the assays used work equally well on a range of household products without background noise causing false readings. To compensate for background noise, we tested two samples.

**Materials and Methods:**

***Instrumentation:***

For detection, we used a detection device made from a rapid manufactured plastic housing that encases simple LEDs and detectors that surround the sample. Detection robustness was achieved by concurrently using UV absorption and fluorescence, as shown in Figure 1 and in the SOM. This detector employs a round geometry allowing simultaneous multi-channel measurement of a baseline and unknown contaminated sample held in standard glass test tubes that cost a few cents each. The detector uses a particularly narrow range of wavelengths relevant to the chemistry one wants to control. For our UV illumination source we chose single-color LEDs in this case, one with an emission peak at 365 nm, in the middle of a broad NADH absorption. For fluorescence illumination we chose a single-color green LED to detect the Amplex Ultrared (Invitrogen) fluorescence. The device had a sensitivity comparable to a commercial plate reader, as was tested by comparing the fluorescence emission from a standard glucose assay in both the device and a commercial plate reader (see SOM). Our detection method was based on comparing sensor output from two samples: one baseline sample made with a known amount of contaminant was held in a 6.5 mm diameter test tube (Durham Culture Tubes 6.50) and one unknown contaminated sample was prepared with an assay or dye and held in a second tube.

***Chemical Methods:***

More detailed chemical methods and protocols may be found in the Supplementary Online Information (SOM).

<u>Ethylene Glycol</u>

Samples, S, containing ethylene glycol (obtained from Sigma Aldrich SAJ first grade) were mixed with household products and medicines at different mass percentages (for details see SOM). To prepare the enzyme stock solutions, an alcohol-dehydrogenase-NAD reagent (A) was made by adding 15 mL of Tris-HCl buffer, pH 8.8, 0.1M (Bio-Rad) to 50 mg NAD (Sigma Aldrich N8535). In mixture B, 0.1 ml of Tris-HCl buffer, pH 8.8, 0.1M (Bio-Rad) was added to 100 mg yeast alcohol dehydrogenase (USB/Affymetrix #10895). To start a sample reaction, 120 µl of the sample, S, were placed in a round 6.50 mm glass tube (Durham Culture Tubes 6.50). Next an enzyme mixture, C, containing 480 µl of solution B and 40 µl of solution A was prepared. All volumes were confirmed by weighing with a scale (Mettler Toledo). To start the reaction in our device, 240 µl of C were added to each tube containing sample, S. A 5.4 wt % EG sample in buffer was always run in parallel as a control.

Diethylene Glycol and Alcohols

Samples, S, of diethylene glycol and alcohols at different mass percentages were prepared in Tris-HCl buffer, pH 7.8, 0.1M (Bio-Rad). Stock solutions A and B (see above) were prepared. In addition stock solutions of 0.05 wt% Amplex Ultrared in DMSO (solution D), 0.044 wt% Horseradish Peroxidase Type 1 (Sigma Aldrich P8125) in Tris-HCl buffer, pH 7.8, 0.1M (solution E), 12 wt% Peroxidase from Enterococcus faecalis (Megazyme, E.C. 1.11.1.1) in phosphate buffer, pH 6.0, 0.1M (solution F) and 0.2 mg/ml Flavin Adenin Dinucleotide (Sigma Aldrich) in deionized water (solution G) were prepared. The final enzyme mixture H contained 480 µl of solution B, 40 µl of solution A and 20 µl each of the solutions D, E, F and G. The reaction was started and read out as described for EG above. For the DEG samples, a reference sample of 5.4 wt % DEG and for alcohols a sample of $5.4 \times 10^{-3}$ wt % was always run in the second chamber as a control.

*Enzyme and pH Optimization*

To screen different alcohol dehydrogenases for their specificity in reacting with DEG we measured the fluorescence product in a plate reader (Molecular Devices) from our assay on 5.4 wt% EG samples in cough syrup and in glycerol, respectively. Pure buffer with one enzyme (USB) was used as a control. The "relative interference" of each enzyme was measured by dividing the initial fluorescence and UV reaction gradient of each sample by the control. The pH of the assay solution was optimized by varying the buffer pH from 6 to 9 and choosing the pH that gives the highest signal-to-noise ratio. The use of NADH oxidase instead of NADH peroxidase made the assay unstable, as NADH oxidase solution decays within minutes at room temperature (see SOM for more detailed methods).

<u>E. Coli, Salmonella and Cholera bacteria in foods and water</u>

We grew cultures of E. Coli (strain: DH5alpha), E. Salmonella (strain: LT2 Delta PhoP/Q S typhi) and Vibrio Cholera (strain: VC O395NT). Bacteria were stained with 2.5 μM Syto 85 (Invitrogen Cat. No. S11366) in deionized water for 3-30 minutes at 250 rpm and 30 °C in the dark; the resulting solutions of stained bacteria are referred to as samples I. The concentration of bacteria in each solution I was measured using the absorption value at 600 nm (Nanodrop 2000). We also stained samples of water (J), milk (K) and egg whites (L) with 2.5 μM Syto 85. Water (J) and milk (K) samples were stained directly as described above. Egg whites (L) were first diluted at a volume ratio 1:1 with deionized water, then vortexed and filtered with a 100 μm filter (BD). The filtrate was centrifuged at 4300 rpm for five minutes and the pellet was reconstituted with water at the same volume of the original egg white sample (L). We now prepared mixtures (M) of stained bacteria (I) with the respective stained products (J, K, L) at different mass fractions. Mass fractions were determined using a scale (Mettler Toledo). To optically measure

M using our detectors, 360 µl of a stained sample mixture M were placed in a round 6.50 mm glass tube (Durham Culture Tubes 6.50). All volumes were confirmed by weighing the samples (Mettler Toledo). A negative, buffer-only control was run in parallel and measured in the detectors. For Sytox Orange staining, cells were lysed using CelLytic (Sigma Aldrich) reagents and stained with 0.1 µM Sytox Orange (Invitrogen Cat. No. S-34861) in TE-buffer for 5 minutes. Further protocols are described in the SOM, particularly those used for the dye optimization procedure.

Yeast in red blood cells (Malaria model)

Baker's yeast (2.86 Mio yeast cells/ml in distilled water) was stained with 5 µM Syto 85 (Invitrogen Cat. No. S11366) in deionized water for 5-60 minutes in the dark. After centrifugation, the bacteria were reconstituted with an equi-volume amount of water in 0.5 g/ml sucrose (yielding solution N). The concentration of bacteria of the resulting solution, N, was measured using the absorption value at 600 nm (Nanodrop 2000). The same procedure was used to stain 2.86 Mio cells/ml bovine red blood cells (Lampire Biologicals #7240807) in sucrose-water, yielding stained solution O. After cell staining, mixtures P containing the components N and O at different mass fractions were prepared utilizing a scale (Mettler Toledo). For the measurement in our device, 360 µl of a stained sample mixture P (prepared above) was placed in a round 6.50 mm glass tube (Durham Culture Tubes 6.50). The volumes were confirmed by weighing the samples (Mettler Toledo). A negative, buffer-only control was run in parallel. For Sytox Orange staining, cells were lysed using CelLytic (Sigma Aldrich) reagents (see SOM) and stained with 0.1 µM Sytox Orange (Invitrogen Cat. No. S-34861) in TE-buffer for 5 minutes. Further protocols are described in the SOM, particularly those used for the dye optimization procedure.

**Results and Discussion:**

***Ethylene Glycol:***

Many reactions involving EG are known; however, those involving enzymes are particularly promising because they offer great specificity and sensitivity. To detect EG, we therefore chose a known, naturally occurring enzymatic reaction where ADH converts a hydroxyl group to an aldehyde and simultaneously converts the coenzyme $NAD^+$ into NADH[5] (Fig. 2A).[37] Hence, the absorption of NADH at 350-370 nm should reflect the concentration of EG.

We illuminated the EG sample with the UV LED and measured the intensity change after the UV light had passed through the liquid EG sample, using a semiconductor light-to-voltage detector, as shown in the schematic in Fig. 1B. To determine $c_\varepsilon$, the mass fraction (concentration) of EG, we added a solution of ADH to the sample, inserted the sample into the sample chamber, and recorded the voltage $V_{ua}(t, c_\varepsilon)$ measured by the UV absorption detector once per second for five minutes (see SOM and Materials and Methods). For pure EG ($c_\varepsilon = 1$), the $V_{ua}(t, c_\varepsilon)$ data fall on a straight line when plotted on a log-log plot, demonstrating a power-law behavior, as shown by the black circles in Fig. 3A. Because the test tube has a circular cross section and the LED has a distribution of illumination angles, a single path-length was not well defined. Therefore, we could not rely on a simple Beer's Law calculation for the absolute absorbance. Instead, we calibrated the device with samples of known $c_\varepsilon$ in water, from the FDA safety limit of $c_\varepsilon = 10^{-3}$ to $c_\varepsilon = 1$.[28] In all cases we observed lines on the log-log plot, $V_{ua}(t, c_\varepsilon) \sim t^{-\gamma(c\varepsilon)}$, as shown with colored symbols in Fig. 3A. The power-law exponent magnitudes $\gamma(c_\varepsilon)$ monotonically increased with $c_\varepsilon$, as shown with the blue circles in Fig. 3B. An optical feedback loop ensured that the LED intensity remained constant irrespective of environmental changes. Thus, there are no adjustable parameters in our determination of $\gamma(c_\varepsilon)$. These data demonstrate our ability to measure $c_\varepsilon$ in

drinking water with a detection limit below 0.1 wt% EG, which has caused sickness and death even in the United States[12], at all concentrations deemed unsafe by the FDA.

Quantifying $c_\varepsilon$ in water, however, does not itself demonstrate the effectiveness of our detection methods in real-world ingestible products and medicines. These have a number of other ingredients that could interfere with the reaction. In particular, most products involved in historical EG poisoning incidents normally have a large fraction of glycerol, propylene glycol or polyethylene glycol.[6,10] These three-carbon glycols have hydroxyl groups that ADH could in principle act upon, altering the measured reaction rate and obscuring the true $c_\varepsilon$. There are a number of ADH variants commercially available. While in general they give similar results for $c_\varepsilon$ in water, subtle differences in structure could have a greater impact in their relative sensitivity to EG in the presence of other glycols. We expected this sensitivity to be even more relevant for DEG (see below), as it is less reactive than EG due to its longer carbon chain. We hypothesized that we could screen the relative interference from glycols in different ADHs. This would allow us to pick the ADH with the least interference from glycols compared with DEG. To investigate the effects of these differences, we screened five different ADH variants for interference by mixing DEG with glycerol, and separately with a mixture containing polyethylene glycol. We then compared the results of the DEG assay described below to the same concentration of DEG in water (see Table 8 in SOM). For our assay we selected the particular ADH variant (USB/Affymetrix) that exhibited the least interference, and we used it in all subsequent measurements.

Using the optimized ADH reaction we detected EG in real-world scenarios, namely household products containing glycols (see Figure 3b). We measured samples with different $c_\varepsilon$ in a variety of unmodified ingestible household products, where contamination has led to historical

poisonings that resulted in fatalities: toothpaste, cough syrup, acetaminophen/paracetamol syrup and antihistamine (allergy) syrup[10]. We chose several name brands and generics of each type, to assure a broad sampling, and repeated the measurements in the same way as for water. Using the optimized ADH assay we found that the $\gamma(c_\varepsilon)$ increases monotonically with $c_\varepsilon$, as in the pure case shown in Fig. 3A. We also observed that the numerical values of $\gamma(c_\varepsilon)$ remain consistent irrespective of the product tested, as shown with colored symbols in Fig. 3B. Each data point is the result of a single measurement. We observed that all data from all products collapse onto a single master curve (with a standard error of 2.58 %), which we indicate with a black line in the figure. By optimizing the ADH enzyme variants we removed any interference from other glycols normally present in the products. This enabled us to achieve universal scaling, with no free fitting parameters, for all products. Our enzyme method can quantify $c_\varepsilon$ at all unsafe levels above the FDA limit of 0.1 wt%, in all real products involved in historical contamination incidents. Our results furthermore suggest that the method could work well even in products where EG contamination has not yet been observed.

***Diethylene Glycol:***

Like EG, DEG poisoning has also killed thousands.[4-21] We therefore repeated the ADH measurements for different DEG concentrations $c_\delta$ in water, expecting it to be less reactive because of the longer carbon chain of DEG compared to EG. Experimentally, we observed DEG to have significantly lower ADH activity, so that we could not distinguish low concentrations of DEG with this simple UV absorption assay alone. We therefore decided to amplify the DEG reaction products by adding enzymatic steps involving fluorescence-based dyes. Fluorescent dyes principally should have a higher signal-to-noise ratio than absorption. Beginning with the

236 ADH reaction, we hence reacted the NADH product with NADH peroxidase and FAD, which
237 generates free radicals that, in the presence of horseradish peroxidase, converts an essentially
238 non-fluorescent resazurin-based dye into a resorufin-based fluorophore[38], as shown in Fig. 1B.
239 However, the pH for maximum activity differs significantly for the different components in the
240 reaction chain: ADH is most active at pH≥8; NADH peroxidase, pH=5; HRP, pH=6-6.5; NAD
241 and FAD, pH=7. It was therefore not obvious that these particular steps could be coupled at a
242 single fixed pH, and still result in detectable fluorophore generation. We investigated this
243 possibility by running the complete reaction chain under a variety of pH conditions (Figure 5a).
244 We found the greatest amount of activity at pH=7.8, which we used for all subsequent
245 measurements. We used NADH peroxidase, rather than NADH oxidase, as the latter solution is
246 unstable and decays within minutes at room temperature (see SOM).
247 Under the optimized assay conditions, a $c_\delta = 1$ sample produced a visible red color change in a
248 few minutes while a $c_\delta = 0$ did not. This result demonstrated, at least qualitatively, the success of
249 the reaction chain in the presence of DEG.
250 To more precisely quantify the progress of this reaction, we added a green LED spaced 60°
251 from the UV LED for excitation, and two additional light detectors, using differently-colored
252 theater gel plastic to filter the green absorption and red fluorescence, placed at 180° and 60°,
253 respectively, relative to the green LED. The round geometry of the sample chamber, as well as
254 offsetting the UV and fluorescence LED activation made this addition possible, without
255 interfering with the existing UV detection scheme. We could thus measure absorption and
256 fluorescence with two excitation wavelengths—which is not possible with a common square
257 cuvette geometry traditionally found in laboratory fluorometers and spectrophotometers.

To measure $c_\delta$ in water, we mixed the enzymes and dye into the sample, and immediately collected voltage data over time from the green and red fluorescence detector, $V_{gf}(t, c_\delta)$. As the reaction proceeded, the increase in fluorescence was manifested as an increase in $V_{gf}(t, c_\delta)$. These data fall onto a straight line when plotted on a semi-log plot, demonstrating the exponential functional form $V_{gf}(t, c_\delta) \sim e^{\nu(c\delta)t}$ as shown in Fig. 4A. We found that the slope of this line, $\nu(c_\delta)$, increases monotonically with $c_\delta$. However, our reaction involves the coupling of three enzymes and a dye, all of which may have slight variations in activity due to environmental factors, which could significantly influence $\nu(c_\delta)$. To account for these variations, we utilized the second, identical sample chamber of the sensor to simultaneously run a 100% DEG sample as a standard reference. Using $\nu_\delta^1 \equiv \nu(c_\delta = 1)$, as a normalization constant, we used the normalized $\nu'(c_\delta) = \nu(c_\delta)/\nu^1_\delta$ to account partially for the effects of variation in total enzyme activity. Furthermore, while collecting $V_{gf}(t,c_\delta)$, the device also collected $V_{ua}(t,c_\delta)$ automatically. This UV data should be sensitive only to the activity of the ADH. Therefore, we calculated the quantity $\gamma'(c_\delta) \equiv \gamma(c_\delta)/\gamma(c_\delta = 1)$, which provides a correction for the variations in absolute ADH activity. Combining the fitted data from the UV- and green-illuminated channels, we observed that $\nu'(c_\delta)\gamma'(c_\delta)$ rises monotonically with $c_\delta$ for DEG in water at all $c_\delta > 0.001$, the FDA safety limit, as shown in Fig. 4B. Each data point in Fig. 4B is the result of at least three independent runs, whose percentage errors decrease with increasing $c_\delta$. The percentage errors are on average 10%, and as low as 3.1% for $c_\delta = 0.25$. As in the EG case, we repeated the measurements for DEG in various household products: once again, we found that the data for some products collapse onto a single curve, though with slightly more scatter than in the EG case, as shown in Fig. 4B. The scatter at each data point decreases from 33% to 1.5% as $c_\delta$ increases from 0.001 to 1. These data

demonstrate our ability to detect DEG, just as for EG, in several ingestible household products and medicines.

The ability to detect these contaminants in remote areas would be greatly enhanced if the chemistry were stable without refrigeration. Indeed, the enzymes and dyes we used are packaged in dry, lyophilized form, and can be shipped overnight without temperature control. How long the activities of these components remain consistent, however, is not well characterized. To test the longer-term stability of our assays, we created large samples with $c_\delta = 0.10$ and $c_\varepsilon = 0.10$, and over the course of several weeks, left all samples, and lyophilized enzymes and dyes at room temperature, without any temperature control. For each measurement, we made a new enzyme solution, and ran the EG and DEG assays. Strikingly, in all cases, the absolute variation in the measured glycol concentrations was less than ±1%, even as the enzymes were at room temperature for more than three weeks, as shown in Fig. 5B. These data demonstrate that our approach to normalizing variations by a combination of LED output stabilization, calibration with reference samples at known concentrations, and combining data from multiple channels, allowed us to eliminate any changes in enzyme activity within our measurement uncertainty. Consequently, our device and chemistry are accurate without requiring a continuous chain of refrigeration (which, for example, is required for immunoassays and other sensitive biochemistry) or other infrastructure, and therefore may be suitable for deployment in disaster areas.

***Alcohols:***

We used ADH to detect glycols that have multiple hydroxyl groups; however, the enzyme originally evolved to convert simple alcohols, with a single hydroxyl group. ADH reacts far

faster with alcohols, and suggests our assay might detect alcohols at far lower concentrations $c_\alpha$. To test this hypothesis, we ran our assay on several alcohols mixed with buffer, including ethanol, 1-propanol, 2-propanol, 1-butanol, 1-pentanol, 1- hexanol, 1-heptanol and 1-octanol. As for the DEG measurement, we calculated $\gamma'$ and $\nu'$ from the UV-and green-illuminated channels, but used $c_\alpha$=0.01 as the reference concentration for each alcohol (instead of $c_\delta = 1$, in the case of DEG). Each data point is the result of at least three independent runs. We observed that the $\gamma'(c_\alpha)\nu'(c_\alpha)$ data for all primary alcohols collapse onto a single master curve, for all $c_\alpha$ above the part-per-billion (ppb) level, as shown in Fig. 6A. The average percentage error between different alcohols at a certain concentration is as low as 7.5% at $c_\alpha = 0.001$. Furthermore, for $c_\alpha = 0.01$, the $\gamma'(0.01)\nu'(0.01)$ data for primary alcohols decreases monotonically with the alcohol carbon number, and is nearly linear within the range of 3 (propanol) to 7 (hexanol) carbons (Fig. 6B). These data demonstrate how our device and chemistry may provide an extremely sensitive probe for the presence of alcohols, and for some primary alcohols, allow them to be identified when concentration is known. For example, this test could be used to detect alcohol in groundwater, which is a sign of gasoline spills or leaks. In addition, we repeated the measurement of ethanol in blood serum, as a way to measure blood alcohol content, shown with hexagons in Fig. 6A. Each data point in Fig. 6 is the result of at least three independent runs. These data overlap the other alcohols exactly for $\gamma'(c_\alpha > 10^{-6})$. We can therefore quantify accurately the $c_\alpha$ for ethanol in blood serum two orders of magnitude below the standard drunk-driving limits of $c_\alpha$ =2 to $8\times10^{-4}$. This method may provide another avenue for rapid, low-cost blood-alcohol measurement in the field, with substantially greater accuracy than breath-based tests.

***Food and Environmental Pathogens:***

The ability to detect transmission and fluorescence from two excitation wavelengths simultaneously allows us to detect a broad range of other chemical reactions or interactions that generate a change in optical activity. For example, we could detect DNA with low-cost intercalator dyes, known to be stable at room temperature for months. This suggested a new use for our system, the detection of microbial DNA, which implies the presence of its host organism, in materials where no DNA should be found, such as recreational water and many foods, where contamination has lead to lethal epidemics. To test our ability to detect such microbial contamination, we mixed different microbial concentrations $c_\mu$ of V. cholera, Salmonella and E. coli bacteria in water, added a DNA intercalator dye, removed free dye, and then measured the final, static green-red fluorescence intensity $V_{gf}^{\infty}(c_\mu) \equiv V_{gf}^{\infty}(t \to \infty, c_\mu)$. The total preparation and measurement time was only a few minutes. In both cases, we found that $V_{gf}^{\infty}(c_\mu)$ rises with $c_\mu >$ $10^5$ CFU/ml (CFU = colony forming units), with a readily discernible detection limit of $10^6$ CFU/ml (based on Kaiser's criterion, see SOM). Our minimum-detectable $c_\mu$ is comparable to total organism concentrations detected in several historical epidemics.[39,40] Furthermore, we tested the concentration of pathogens in pond water (Bow, New Hampshire) and measured a baseline activity indistinguishable from background levels in doubly distilled water. These data demonstrate the utility of our method to potentially preventing recreational water epidemics, where fast turnaround times may be desirable. Even though the methods introduced here can detect bacteria at concentrations found in several historical epidemics[39,40], lower detection limits may be desirable since the presence of as low as 10 cells of Salmonella or E. coli O157:H7 may be an infectious dose[41]. The EPA recommendation for recreational waters is around 1 CFU/ml[42], even though higher detection limits may be acceptable, especially where fast turn-around times

348 are needed. To increase detection sensitivity we optimized the fluorescent dyes and used lysed
349 cells rather than whole cells, where the DNA is expected to be more accessible to the dyes. As
350 shown in Figure 8 we achieved a readily discernible detection limit of $c_\mu = 10^4$ CFU/ml (based on
351 Kaiser's criterion), by lysing the cells and using the DNA dye Sytox Orange rather than Syto 85.
352 Sytox Orange was chosen, as it is compatible to the current optical setup of the device. Further
353 optimization of dyes and lysis conditions could improve this detection limit even more (see SOM
354 part G).

355 Another major area where DNA should not be present is in foods that do not contain cellular
356 tissue from animals or plants. Many of these, such as milk and eggs, have been involved in
357 massive food poisoning outbreaks when contaminated by bacteria such as E. coli or E.
358 Salmonella.[22,25] Unlike drinking water, however, these complex biological materials contain
359 other components with the potential to interfere with the DNA intercalator dyes. To test our
360 ability to quantify microbial contamination in these materials, we repeated the above procedure
361 with E. coli in milk, and E. salmonella in egg white, combinations that have caused lethal food
362 poisoning in the past. Once again, in both cases, $V_{gf}^{\infty}(c_\mu)$ rose with $c_\mu$. However, the curves of
363 $V_{gf}^{\infty}(c_\mu)$ for the four bacterial data sets did not overlap on the same curve, possibly due to
364 differences in auto fluorescence of the materials and foods. With a traditional fluorometer, little
365 could be done without further sample modifications. The multichannel design of our detector,
366 however, gave us a number of additional options, since we also collected automatically the final,
367 static green absorption $V_{ga}^{\infty}(c_\mu)$ and UV→ red fluorescence $V_{uf}^{\infty}(c_\mu)$. We searched for
368 combinations of channel metrics for which all four bacteria collapsed onto the same master
369 curve. By trial, we found universal data collapse for the normalized multichannel metric

370 $V_{gf}^{\infty}(c_\mu)\sqrt{(V_{uf}^{\infty}(c_\mu)\cdot V_{ga}^{\infty}(c_\mu)}$, as shown in Fig. 7A. Again, using Syto 85 we found that

371 $V_{gf}^{\infty}(c_\mu)\sqrt{(V_{uf}^{\infty}(c_\mu)\cdot V_{ga}^{\infty}(c_\mu)}$ rises with $c_\mu > 10^5$ CFU/ml, with a readily discernible detection limit

372 of $10^6$ CFU/ml (Kaiser's criterion). Given the similar spectral characteristics, we expect that

373 using Sytox Orange would further reduce the detection limit to $c_\mu \sim 10^4$ CFU/ml as in the case of

374 pure bacteria shown in Figures 8 A and B.

375 These data demonstrate how our device can be used in a general way to measure microbial

376 concentration in substrates that should not contain DNA, irrespective of particular bacteria or

377 substrate. This is particularly important in foods and medicines, where a wide range of bacteria

378 are known to cause poisoning.[25,26] We emphasize that our measurements were taken directly on

379 samples and require only a few minutes of dye exposure. Our results were unchanged while

380 varying dye incubation times from 3 to 30 minutes (see SOM), in contrast to the hours or days

381 required for culturing or PCR analysis[36]. Our detection limit of $10^4$ CFU/ml is comparable to

382 most electrical, electrochemical (e.g. impedance, DEP) and immunochemical biosensors, which

383 usually have detection limits between $10^3$ and $10^5$ CFU/ml with an assay time of at least two

384 hours under ideal conditions[43-47]. Other optical methods (e.g. SPR, IR, optical fibers etc.) may

385 achieve even lower detection limits, but often require several hours[43] and/ or cost around 2 orders

386 of magnitude more than the sensor described here[41,48]. Traditional methods (such as cell culture,

387 PCR or ELISAs) have lower detection limits between $10^1$ and $10^6$ CFU/ml. However, they

388 require incubation of several hours (PCR 4-6 hrs) to days (culture methods up to 5-7 days), as

389 well as a stable laboratory environment often in combination with expensive equipment.[41] The

390 introduced detection scheme may therefore be used as a simple, low-cost first screen and line of

391 defense for pathogen contamination in a range of consumer products, recreational water,
392 medicines and food products.

393 **Blood-borne pathogens (e.g. malaria):**

394 In addition to prokaryotes, we could apply the same method to a eukaryotic biological system
395 where the presence of DNA indicates the presence of pathogenic microbial invasion. Several
396 blood-borne pathogens, for example malaria-causing plasmodium, invade red blood cells
397 (RBCs), which have no DNA of their own. Moreover, RBCs can be separated from other DNA-
398 bearing cells in blood using existing low-cost methods[49]. It might thus be possible for our
399 methodology to detect this type of parasitic blood infection. To test this concept qualitatively, we
400 created a rudimentary model for malarial invasion by dyeing suspensions of yeast with Syto 85,
401 which we chose because they are safe to handle and have a total genome size about half that of
402 plasmodium. We dyed yeast both in water, and mixed with red blood cells as a model for
403 malaria. After a brief incubation, we measured fluorescence and absorption, following the
404 protocol as for bacteria. As in the bacterial case, when using fluorescence or absorption alone,
405 different data sets scaled differently. In particular, the data for yeast in red blood cells did not
406 overlap that for yeast in water. We therefore combined the different parameters until we
407 achieved universal data collapse. We found that, when normalizing the green→red fluorescence
408 intensity by the cube of the green absorption, $V_{gf}^{\infty}(c_{\mu})/V_{ga}^{\infty}(c_{\mu})^3$, the data from both sets fall onto
409 the same curve—and at low concentrations asymptote to the baseline value we measure for red
410 blood cells alone, as shown in Fig. 7B. Again, using Syto 85 we found that $V_{gf}^{\infty}(c_{\mu})/V_{ga}^{\infty}(c_{\mu})^3$ rises
411 with $c_{\mu}$ at a detection limit of $c_{\mu} > 8 \cdot 10^5$ CFU/ml (based on Kaiser's criterion). The detection
412 limit could again be improved by using lysed cells and the DNA-dye Sytox Orange instead of

Syto 85. We therefore stained pure, lysed yeast cells with Sytox Orange, where we achieved a detection limit of $c_\mu \sim 10^4$ CFU/ml as for the tested bacteria (see Fig. 8b). These preliminary data demonstrate that the intercalator has no significant background interference from residual RNA or ribosomal nucleotides in the red blood cells. Therefore, our method has the potential to quantify rapidly in RBC suspensions the concentration of blood-borne DNA-bearing parasites, such as plasmodium (malaria), trypanosoma (sleeping sickness and chagas) and the eggs of trematodes (schistosomiasis).

In this paper, contaminants were detected directly in various substances, without separation, purification, concentration or incubation. New enzyme- and dye-based methods to detect (di-)ethylene glycol in consumables above 0.1 wt% without interference and alcohols above 1 ppb were introduced. Using DNA intercalating dyes a range of pathogens in water, foods and blood were detected without background signal at a detection limit of $10^4$ CFU/ml. The detection scheme uses fluorescence and/or UV absorption measurements made on samples in a small round test tube. Our simple system makes practical the multiple channels and samples that allow us to normalize by references and combine data from different simultaneous measurements. The individual channels within our detector have sensitivities comparable to commercial optical laboratory instruments costing significantly more. In addition, contaminant concentrations we measured did not change with background substrate, which demonstrates that our detection methods are broadly effective in a wide variety of substances, and could apply in a general way to new substances where contamination might not yet have been found.

We emphasize that we have but scratched the surface of this exciting area, and our preliminary results can be improved and extended in many ways. We have examined a limited number of contaminants, but our strategy should be applicable to any chemical reaction that in the

436 presence of a contaminant leads to a change in optical activity. For example, commercial kits are
437 available that use a fluorescence-generating reaction to detect melamine in milk products.
438 The effective detection sensitivity of our scheme could be improved by dye optimization,
439 concentration of microorganisms through mechanical methods such as filtering, or where time is
440 not a factor by incubation at elevated temperatures. The sensitivity could be further improved by
441 adding a third LED or by optimizing LEDs, filter specifications and excitation and emission
442 times to the specific dye used. Moreover, for bacterial detection, we chose a non-specific DNA
443 intercalator dye because of its extremely low cost and high stability, but as a result our assay is
444 insensitive to the actual genome being detected and the sensitivity is limited. In many situations,
445 where continuous refrigeration is available and cost pressure is not so severe, more specific
446 biochemical tagging (e.g. molecular beacons), DNA amplification (isothermal or PCR) or
447 immunoassays (e.g. antibodies, ELISAs) could be used to increase detection sensitivity and/ or to
448 detect the presence of specific, targeted pathogens.
449 Our chemistry is stable for weeks without refrigeration and the rapid detection time of our
450 assays allows testing of perishable foods and ingestible products, which often are not tested
451 because current culturing-based methods require multiple days. The device we created is also
452 robust and simple-to-use. In the future it could be run on batteries and a smart mobile-phone/
453 tablet platform could be used to aggregate data for use in remote areas. One could also envisage
454 a device consisting of LEDs or a simple number readout that gives the end-user a simple yes or
455 no answer of whether the sample is contaminated (as indicated in Fig. 1).
456 This new capability may have potential applications in much broader sampling of both
457 domestic and imported foods and agricultural products, enabling end-to-end characterization
458 within a food or medicine supply chain. By leveraging amplification methods and existing

chemical labeling technologies to identify the presence of chemical and biological contaminants, we hope that our work might be a first step towards preventing many diseases and deaths.

## ABBREVIATIONS USED.

Ethylene Glycol (EG); Diethylene Glycol (DEG); Alcohol Dehydrogenase (ADH); Nicotinamide Adenine Dinucleotide (NAD); Flavin Adenine Dinucleotide (FAD), Horseradish Peroxidase (HRP), Colony Forming Units (CFU).

## ACKNOWLEDGMENT.

We thank Hong Ma, J. Voldman, the CR/ARY 2 team at Robert Bosch GmbH (particularly J. Steigert, B. Faltin and P. Rothacher), S. Finch, L. Przybyla, M. Vahey, D. Markus, J. Helferich and B. Stupak for their contributions and guidance.

## SUPPORTING INFORMATION AVAILABLE.

1) Recent contamination incidents leading to sickness, hospitalization and death 2) Detailed Materials and Methods.

REFERENCES.


1. United States House or Representatives Subcommittee on Science and Technology, **2007**. FDA: Science and Mission at Risk. *Report of the Subcommittee on Science and Technology.* Available: http://www.fda.gov/ohrms/dockets/ac/07/briefing/2007-4329b_02_01_FDA%20Report%20on%20Science%20and%20Technology.pdf [accessed 20. May 2011].

2. Sack, K.; Williams, T. Deaths of 9 Alabama patients tied to intravenous supplement. *N. Y. Times* **2011**, 30 Mar.

3. Tagliabue, J. Scandal over poisoned wine embitters village in Austria. *N. Y. Times* **1985**, 2 Aug.

4. Bogdanich, W.; Hooker, J. Toxic Toothpaste Made in China is found in the U.S. *N. Y. Times* **2007***,* 6 May.

5. Gomes, R.; Liteplo, R.; Meek, M. E. Ethylene glycol: human health aspects. *World Health Organization* **2002**.

6. ATSDR (U.S. Department of Human Health and Services, Agency for Toxic Substances and Disease Registry), **2010**. Toxicological Profile for Ethylene Glycol. Available: http://www.atsdr.cdc.gov/toxprofiles/tp96-c7.pdf [accessed 20. May 2011]..

7. Schep, L. J.; Slaughter, R. J.; Temple, W. A.; Beasley, D. M. G. Diethylene glycol poisoning. *Clin. Tox.* **2009**, 47, (6), 525-535.

8. Schier, J.; Conklin, L.; Sabogal, R.; Dell'Aglio, D.; Sanchez, C.; Sejvar, J. Medical toxicology and public health—Update on research and activities at the centers for disease

control and prevention and the agency for toxic substances and disease registry. *J. Med. Tox.* **2008**, 4, (1), 40-42.

9. Wax, P. M. Elixirs, diluents, and the passage of the 1938 Federal Food, Drug and Cosmetic Act. *Ann. Intern. Med.* **1995**, 122, (6), 456.

10. SCCP (European Commission Scientific Committee on Consumer Products), **2008**. Opinion on Diethylene Glycol. Available: http://ec.europa.eu/health/ph_risk/committees/04_sccp/docs/sccp_o_139.pdf [accessed 20. May 2011].

11. Leikin, J.B.; Toerne, T.; Burda, A; McAllister, K.; Erickson, T. Summertime cluster of intentional ethylene glycol ingestions. *J. Amer. Med. Assn.* **1997**, 278, 1406.

12. Schultz, S.; Kinde, M.; Johnson, D. Ethylene glycol intoxication due to contamination of water systems. *Morb Mortal Wkly Rep* **1987**, 36, 611-614.

13. United States Environmental Protection Agency, **2001**. Potential Contamination Due to Cross-Connections and Backflow and the Associated Health Risks, Office of Ground Water, *EPA Distribution System Issue Paper.* Available: http://www.epa.gov/ogwdw/disinfection/tcr/pdfs/issuepaper_tcr_crossconnection-backflow.pdf [accessed 20. May 2011].

14. Abubukar, A.; Awosanya, E.; Badaru, O.; Haladu, S.; Nguku, P.; Edwards, P.; Noe, R.; Teran-Maciver, M.; Wolkin, A.; Lewis, L. Fatal poisoning among young children from diethylene glycol-contaminated acetaminophen-Nigeria, 2008-2009. *Morb. Mortal. Wkly. Rep.* **2009**, 58, (48), 1345-1347.

15. Singh, J.; Dutta, A. K.; Khare, S.; Dubey, N. K.; Harit, A. K.; Jain, N. K.; Wadhwa, T. C.; Gupta, S. R.; Dhariwal, A. C.; Jain, D. C. Diethylene glycol poisoning in Gurgaon, India, 1998. *Bull. W H O* **2001**, 79, 88-95.

16. O'Brien, K. L.; Selanikio, J. D.; Hecdivert, C.; Placide, M. F.; Louis, M.; Barr, D. B.; Barr, J. R.; Hospedales, C. J.; Lewis, M. J.; Schwartz, B. Epidemic of pediatric deaths from acute renal failure caused by diethylene glycol poisoning. *Amer. Med. Soc.* **1998**, 279, (15), 1175.

17. Hanif, M.; Mobarak, M. R.; Ronan, A.; Rahman, D.; Donovan Jr, J. J.; Bennish, M. L. Fatal renal failure caused by diethylene glycol in paracetamol elixir: the Bangladesh epidemic. *Brit. Med. J.* **1995**, 311, (6997), 88.

18. Okuonghae, H. O.; Ighogboja, I. S.; Lawson, J. O.; Nwana, E. J. Diethylene glycol poisoning in Nigerian children. *Ann. Trop. Paediatr.* **1992**, 12, (3), 235.

19. Pandya, S. K. Letter from Bombay. An unmitigated tragedy. *Brit. Med. J.* **1988**, 297, (6641), 117

20. Wax, P. M. It's happening again—another diethylene glycol mass poisoning. *Clin. Toxicol.* **1996**, 34, (5), 517-520.

21. Osterberg, R. E.; See, N. A. Toxicity of excipients—A Food and Drug Administration perspective. *Int. J. Toxicology* **2003**, 22, (5), 377.

22. Scallan, E.; Hoekstra, R. M.; Angulo, F. J.; Tauxe, R. V.; Widdowson, M. A.; Roy, S. L.; Jones, J. L.; Griffin, P. M. Foodborne illness acquired in the United States—major pathogens. *Emerg. Infect. Dis.* **2011**, 17, 7.

23. CDC (Centers for Disease Control and Prevention) **2011**. Salmonella Outbreaks http://www.cdc.gov/salmonella/outbreaks.html [accessed 20. May 2011].

24. CDC (Centers for Disease Control and Prevention) **2011**. Outbreak Investigation of E. Coli http://www.cdc.gov/ecoli/outbreaks.html [accessed 20. May 2011].

25. Mead, P. S.; Slutsker, L.; Dietz, V.; McCaig, L. F.; Bresee, J. S.; Shapiro, C.; Griffin, P. M.; Tauxe, R. V. Food-related illness and death in the United States. *Emerg. Infect. Dis.* **1999**, 5, (5), 607.

26. Griffith, D. C.; Kelly-Hope, L. A.; Miller, M. A. Review of reported cholera outbreaks worldwide, 1995-2005. *Am. J. Trop. Med. Hyg.* **2006**, 75, (5), 973.

27. Theron, J.; Cilliers, J.; Du Preez, M.; Brözel, V. S.; Venter, S. N. Detection of toxigenic Vibrio cholerae from environmental water samples by an enrichment broth cultivation–pit stop semi nested PCR procedure. *J. Appl. Microbiol.* **2000**, 89, (3), 539-546.

28. United States Food and Drug Administration, **2010**. Guidance for Industry: Testing of Glycerin for Diethylene Glycol. Available: http://www.fda.gov/downloads/Drugs/GuidanceComplianceRegulatoryInformation/Guidances/ucm070347.pdf [accessed 20. May 2011]

29. Leonard, P.; Hearty, S.; Brennan, J.; Dunne, L.; Quinn, J.; Chakraborty, T.; O'Kennedy, R. Advances in biosensors for detection of pathogens in food and water. *Enzyme and microbial technology* **2003**, 32, (1), 3-13.

30. Nugen, S. R.; Baeumner, A. J. Trends and opportunities in food pathogen detection. *Anal. Bioanal. Chem* . **2008**, 391, (2), 451-454.

31. Velusamy, V.; Arshak, K.; Korostynska, O.; Oliwa, K.; Adley, C. An overview of foodborne pathogen detection: in the perspective of biosensors. *Biotech. Adv.* **2010**, 28, (2), 232-254.

32. Kenyon, A. S.; Shi, X.; Wang, Y. A. N. Simple, at-site detection of diethylene glycol/ethylene glycol contamination of glycerin and glycerin-based raw materials by thin-layer chromatography. *J. AOAC Intl.* **1998**, 81, (1), 44-50.

33. Yager, P.; Domingo, G. J.; Gerdes, J. Point-of-care diagnostics for global health. *Annu. Rev. Biomed. Eng.* **2008**, 10, 107-144.

34. Kost, G. J. Newdemics, public health, small-world networks, and point-of-care testing. *Point of Care* **2006**, 5, (4), 138.

35. Fukushima, H.; Tsunomori, Y.; Seki, R. Duplex real-time SYBR green PCR assays for detection of 17 species of food-or waterborne pathogens in stools. *J. Clin. Microbiol.* **2003**, 41, (11), 5134.

36. Yasmin, M.; Kawasaki, S.; Kawamoto, S. Evaluation of Multiplex PCR System for Simultaneous Detection of Escherichia coli O157: H7, Listeria monocytogenes and Salmonella enteritidis in Shrimp Samples. *Bangl. J. Microbiol.* **2008**, 24, (1), 42-46.

37. Eckfeldt, J. H.; Light, R. T. Kinetic ethylene glycol assay with use of yeast alcohol dehydrogenase. *Clin. Chem.* **1980**, 26, (9), 1278.

38. Batchelor, R. H.; Zhou, M. A resorufin-based fluorescent assay for quantifying NADH. *Anal. Biochem.* **2002**, 305, (1), 118.

576 39. Gadgil, A. Low cost UV disinfection system for developing countries: field tests in South
577 Africa. *Ann. Rev, Energy and Env. Fed.* **1998**, 23, 253.

578 40. Danley, A. A.; Watts, M. J. Installation of Bio-Sand Filters in Petite Paradise, Haiti.
579 *Proc. Water Env. Fed.* **2009**, (12), 3892-3897.

580 41. Lazcka, O.; Del Campo, F.; Munoz, F. Pathogen detection: a perspective of traditional
581 methods and biosensors. *Biosens. Bioelectron.* **2007**, 22, 1205–1217.

582 42. Noble, R.; Weisberg, S. A review of technologies for rapid detection of bacteria in
583 recreational waters. *J Water Health* **2005**, 03, 381-392.

584 43. Yan, L; Bashir, L. Electrical/electrochemical impedance for rapid detection of foodborne
585 pathogenic bacteria. Biotech. Adv. 2008, 26, 135–150.

586 44. Ivnitsk, D.; Abdel-Hamid, I;, Atanasov, P.; Wilkins, E. Biosensors for detection of
587 pathogenic bacteria. *Biosens Bioelectron* **1999**,14,599–624.

588 45. Ivnitsk, D.; Abdel-Hamid, I.; Atanasov, P.; Wilkins, E.; Stricker, S. Application of
589 electrochemical biosensors for detection of food pathogenic bacteria. *Electroanal*. **2000**,
590 12, 317–25.

591 46. Su, X.L.; Li, Y. A self-assembled monolayer-based piezoelectric immunosensor for rapid
592 detection of Escherichia coli O157:H7. *Biosens. Bioelectron.* **2004**, 19,(6), 563–74.

593 47. Rand, A.G.; Ye, J.; Brown, C.W.; Letcher, S.V. Optical biosensors for food pathogen
594 detection. *Food Tech.* **2002**, 56, (3), 32–9.

595 48. Personal communication and price enquiry with manufacturers.

49. Sriprawat, K.; Kaewpongsri, S.; Suwanarusk, R.; Leimanis, M. L. Effective and cheap removal of leukocytes and platelets from Plasmodium vivax infected blood. *Malaria journal* **2009**, 8, (1), 115.

FUNDING:

This work was supported by CIMIT, the Legatum Center at MIT, Robert Bosch GmbH and Prof. Slocum's Pappalardo Chair discretionary funds.

CONFLICT OF INTEREST:

The authors declare no competing financial interest.

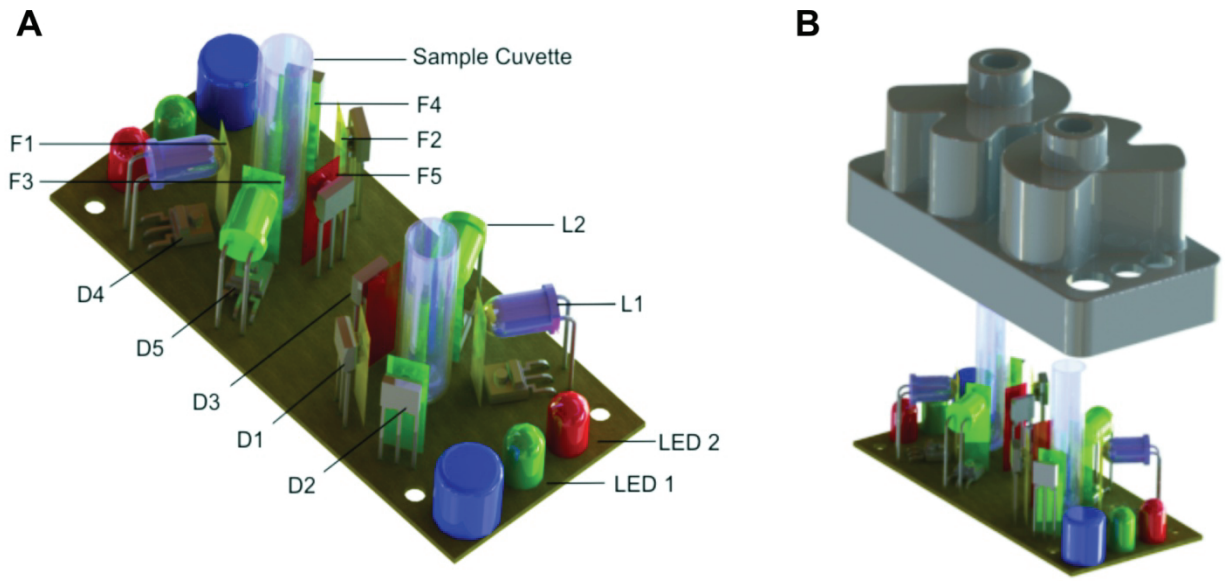


**Figure 1.** Schematic overview and rendering of our multi-channel, multi-sample (baseline and prepared) UV/vis absorption and fluorescence detector. **(A)** Interior device electronics. UV light emitted by an LED (L1) passes through an excitation filter (F1), the sample, and another filter (F2) before absorption is detected (D1). Detector DF1 provides a feedback signal to an op-amp that maintains constant light output from L1, whose baseline level is set by a microcontroller. Light from a similarly stabilized green LED (L2) is filtered (F3) before passing through the sample. Green light is filtered and detected for green absorption (F4, D2) and red fluorescence (F5, D3). Voltage outputs from the detectors (D1, D2, D3) are digitized and sent from a microcontroller to an external computer. LED 1 ("yes") and LED 2 ("no") are simple light-readouts telling the end-user whether the sample is contaminated or not (LED1 and LED2 are design suggestions and have not been integrated into the used prototype). **(B)** To assemble a device, two mirror image enclosure units are snapped together and placed over the circuit board containing the LEDs and detectors. The optical setup and electronics are precisely aligned in the

enclosure by flexural springs molded into the cover, which force the components against reference features.

| Contaminant | Contaminated materials | Detection Mechanism | Spectral Range |
|---|---|---|---|
| **Ethylene Glycol** | Consumer household products and medicines | Enzymatic | UV |
| **Diethylene Glycol** | Consumer household products and medicines | Enzymatic | Fluor-escence + UV |
| **Alcohols** | Groundwater | Enzymatic | Fluoresc. + UV |
| **Food Pathogens** | Foods, e.g. milk, eggs, cider | DNA dye | Fluor-escence |
| **Environmental Pathogens** | (Recreational) Water | DNA dye | Fluor-escence |
| **Bloodborne Pathogens** | Blood | DNA dye | Fluor-escence |

**Table 1.** Applications for detecting poisons, contaminants and pathogens and their detection mechanisms.

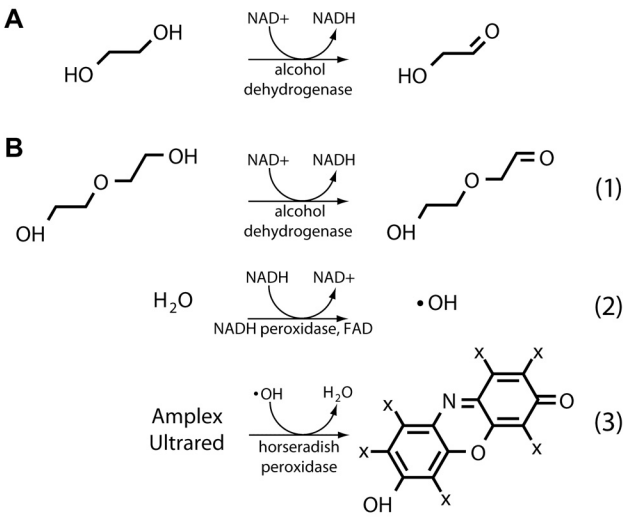


**Figure 2.** Chemical reactions. (**A**) ADH converts EG to an aldehyde in the presence of NAD+, which is converted to NADH; we measured the increase in NADH concentration with our UV absorption detector. (**B**) The DEG reaction begins with the same first step (A), but instead of detecting NADH directly, NADH peroxidase converts NADH back to NAD+ with an FAD coenzyme. This reaction generates hydrogen peroxide, which forms radicals that convert a resazurin-based dye into its fluorescent form. We detected the increase in fluorophore concentration with our fluorescence detector.

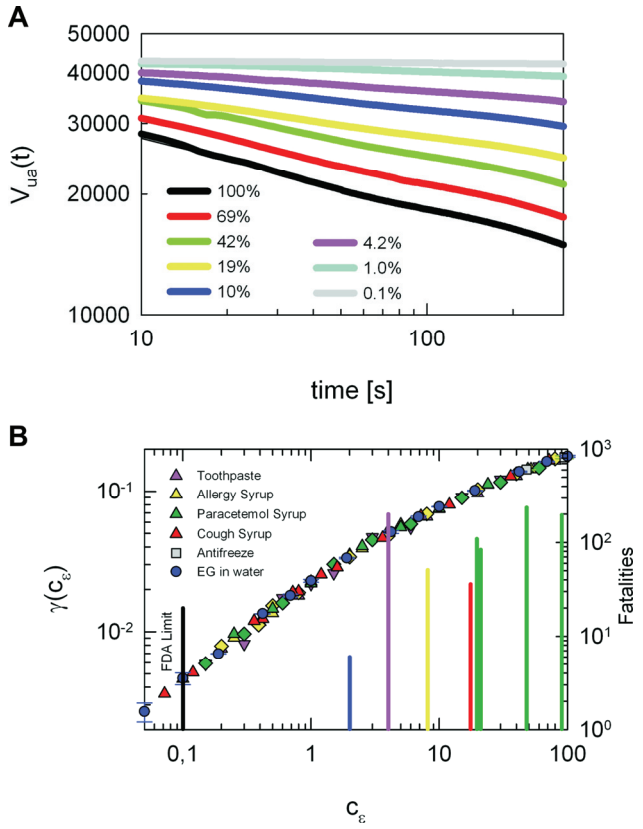


**Figure 3.** Detection of ethylene glycol contamination using UV absorption. **(A)** Time evolution of output voltage $V_{ua}(t)$ from the UV detectors, digitized as 16-bit integer, shown on a log-log plot with symbols for different EG concentrations $c_\varepsilon$ in water. The data fall onto a straight line for each sample, demonstrating power-law scaling. **(B)** The magnitude of the slope of each line $\gamma(c_\varepsilon)$ varies monotonically with $c_\varepsilon$, shown with blue circles for pure EG. The $\gamma(c_\varepsilon)$ values for a variety of different household products (colored triangles) and antifreeze (squares) all fall onto the same master curve, shown in black as a guide to the eye, demonstrating a universal scaling of this measure of EG concentration, irrespective of product contaminated. FDA safety limit $c_\varepsilon = 10^{-3}$ is indicated with a grey vertical line. EG concentrations of historical epidemics are indicated with bars whose color indicates the type of product contaminated, following the same color scheme as the data points; the number of deaths in each incident is represented by the height of the bar, indicated on the right-hand vertical axis.

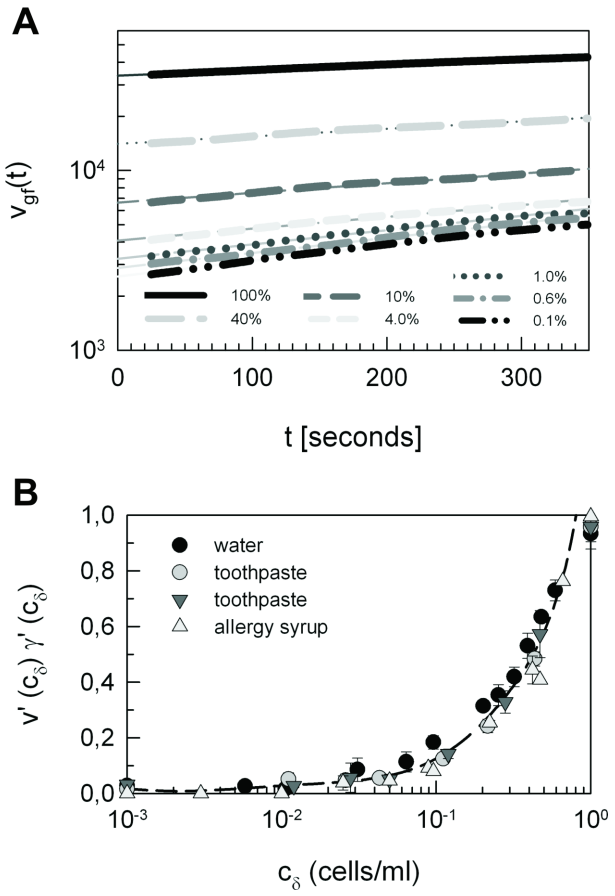


**Figure 4.** Detection of diethylene glycol using a combination of green→red fluorescence and UV absorption. **(A)** Time evolution of output voltage $V_{gf}$ (t) from the green→red fluorescence detector, digitized as 16-bit integer, shown on a semi- log plot with symbols for different DEG concentrations in water; the data fall onto a straight line for each sample, indicating exponential behavior. **(B)** Combination of normalized UV absorption and green→red fluorescence data, $\nu'(c_\delta)\gamma'(c_\delta)$, shown with solid black circles for DEG in water; data for other ingestible household products (other symbols) fall on the same master curve (dashed line).

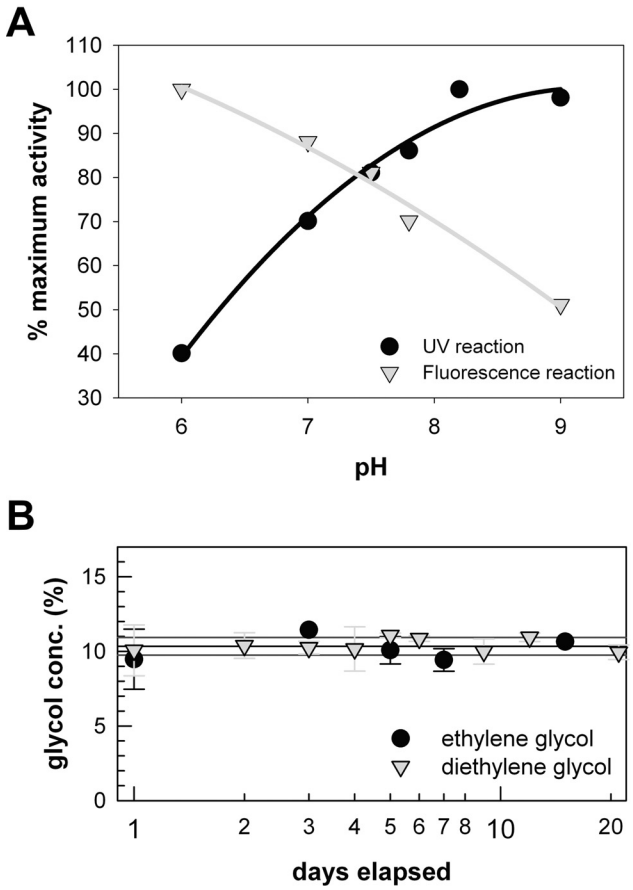


**Figure 5. (A)** pH optimization of the DEG assay: By varying the buffer pH from 6 to 9 we observe the highest overall signal-to-noise levels between pH 7.5-8, where both fluorescence absorption are at a high percentage of their maximum activity. **(B)** Assay stability measurement using the same $c_\delta = 0.1$ (DEG) and $c_\varepsilon = 0.1$ (EG) samples over time, with enzymes left to sit at room temperature. Average and standard deviation of measurements are marked with solid and dotted lines, respectively. In all cases, the measured glycol concentrations remained stable to within ±1% throughout the course of more than three weeks.

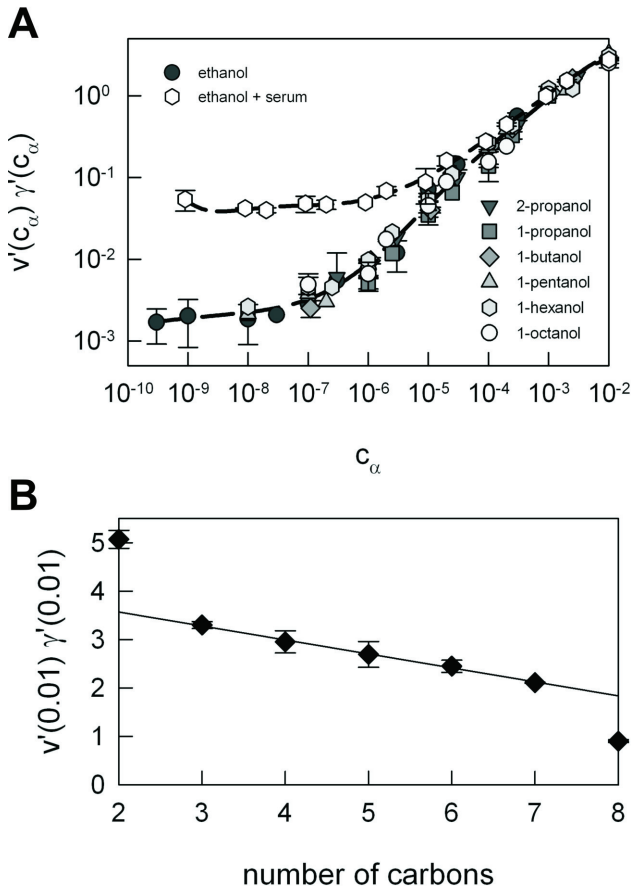


**Figure 6**. Detection and characterization of alcohols. **(A)** Combination of normalized UV absorption and green→red fluorescence data, $\nu'(c_\alpha)\gamma'(c_\alpha)$, for various alcohols in water, as a function of concentration $c_\alpha$. The data collapse onto a single master curve, marked with a black curve, for all concentrations greater than a few parts per billion. Data for ethanol in blood serum plateaus to a background of a few parts per million, well below the legal blood-alcohol limits in a variety of countries, which range from 2 to $8 \times 10^{-4}$. **(B)** Absolute value of $\nu'(0.01)\ \gamma'(0.01)$ for primary alcohols, which decreases monotonically with increasing carbon number. For alcohols with 3 to 7 carbons, this decrease is linear, marked with a solid line.

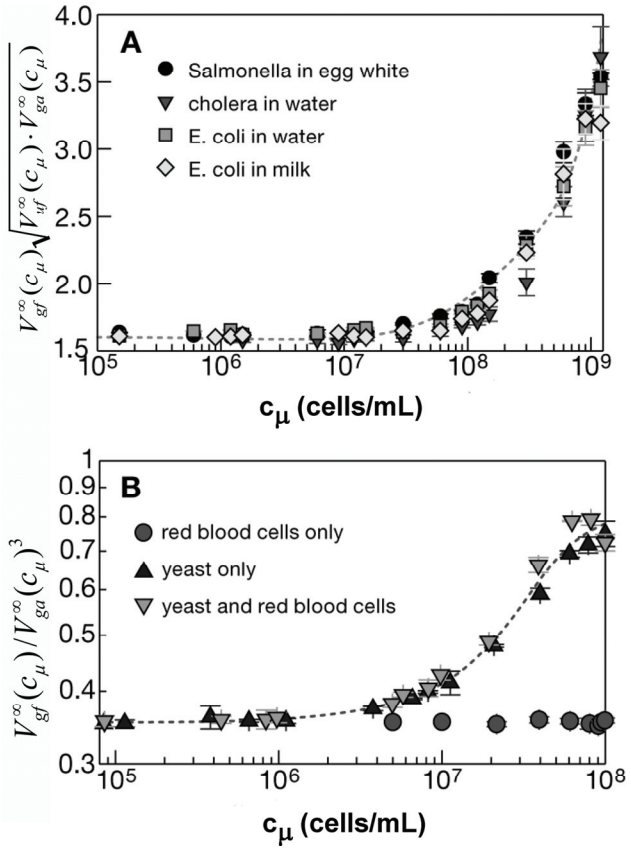


**Figure 7.** Detection of microbial contamination. **(A)** Combined normalized multi-channel data $V_{gf}^{\infty}(c_\mu)\sqrt{V_{uf}^{\infty}(c_\mu)\cdot V_{ga}^{\infty}(c_\mu)}$ from DNA intercalator dye in the presence of prokaryotic pathogens at different concentrations $c_\mu$. In all cases, the data from cholera in water, E. coli in water and in milk, and salmonella in egg white, all collapse onto the same master curve (dotted line). This demonstrates universal, species-independent behavior of our bacterial detection scheme. **(B)** Rudimentary model for the detection of eukaryotic blood parasites, such as malaria. Combined normalized multichannel data $V_{gf}^{\infty}(c_\mu)/V_{ga}^{\infty}(c_\mu)^3$ for dyed yeast both in water (grey triangles) and in red blood cells (inverted, grey triangles) scale onto the same master curve (dotted line), and at low concentration plateau to the background sample of red blood cells alone (circles).

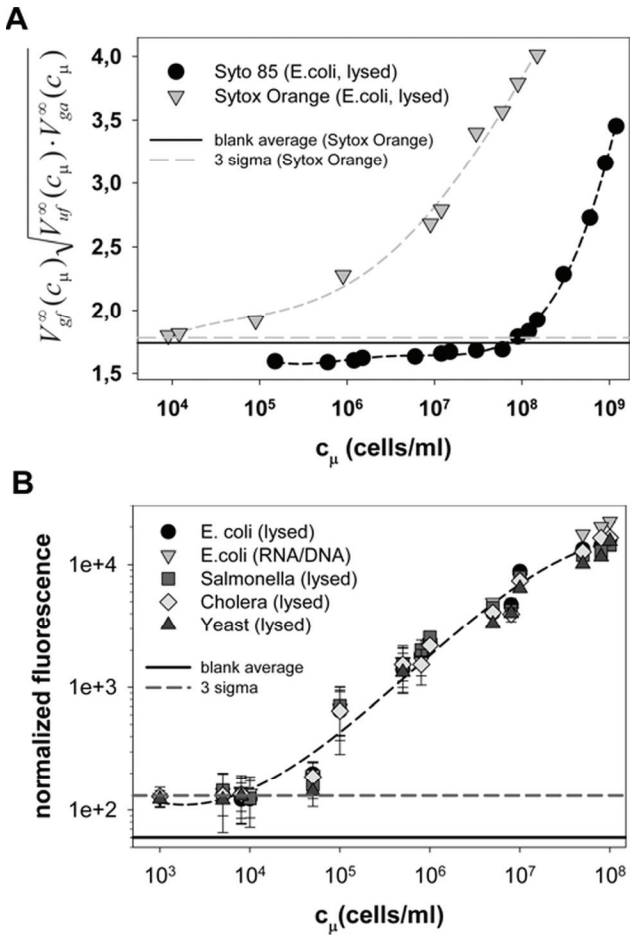


**Figure 8:** Dye optimization **(A)** Comparison of Sytox Orange and Syto 85 detection limits. Shown are the combined normalized multi-channel data $V_{gf}^{\infty}(c_\mu)\sqrt{V_{uf}^{\infty}(c_\mu)\cdot V_{ga}^{\infty}(c_\mu)}$ from DNA intercalator dyes in the presence of E. coli cells at different concentrations $c_\mu$. Using Sytox Orange with lysed E.coli cells improves the detection limit to $c_\mu = 10^4$ CFU/ml, compared with $10^6$ CFU/ml in Syto 85. **(B)** Validation of Sytox Orange staining for different bacteria (Salmonella, Cholera, E.coli) and yeast. This graph shows Sytox Orange stained lysed bacteria and lysed yeast cells at different concentrations measured in a plate reader (whose sensitivity is comparable to the used device, see SOM) . The fluorescence values are normalized by the pathogen genome size and are the the averages of three independent runs. A detection limit of $c_\mu$

= $10^4$ CFU/ml (based on Kaiser's 3δ criterion) was achieved for all bacteria, demonstrating that Sytox Orange will improve the detection limit for all tested pathogens.

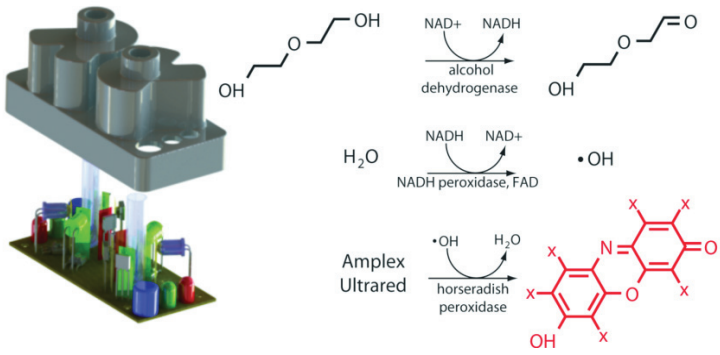
OH
O
OH
NAD+
NADH
alcohol
dehydrogenase
O
O
OH
H2O
NADH
NAD+
NADH peroxidase, FAD
•OH
Amplex
Ultrared
•OH
H2O
horseradish
peroxidase
X
X
X
N
O
X
X
X
OH
O

**TOC Figure**